

DISCOVERY OF A LIGHT ECHO FROM SUPERNOVA 2003GD

BEN E.K. SUGERMAN

Space Telescope Science Institute, 3700 San Martin Dr., Baltimore, MD 21286 U.S.A.

Accepted 2005 Aug 30 by the *Astrophysical Journal Letters*

ABSTRACT

Archival *HST*/ACS data reveal details of a light echo around SN 2003gd in the galaxy M74, only the fifth supernova around which resolved echoes have been reported. An echo is detected $0.''3$ from the supernova between PA 250° – 360° , with fainter signal present at a few other position angles. This material lies ~ 180 pc in front of the supernova, with a thickness of 60–120 pc, and may delineate the disk of M74. This structure has a gas density of 1 – 2 cm $^{-3}$, typical of the interstellar medium, however, the dust grains are smaller than those found in our Galaxy, with maximum grain sizes around $0.25\mu\text{m}$. Since only one epoch of data exists, in two wavebands and with low signal-to-noise, deeper, annual visits should be made with *HST* and ground-based adaptive optics telescopes.

Subject headings: supernovae: individual (SN 2003gd) — ISM: structure — galaxies: individual (NGC 628) — reflection nebulae

1. INTRODUCTION

Supernova (SN) 2003gd was discovered by Evans & McNaught (2003) on 2003 June 12.8 in a southern spiral arm roughly $151'$ from the nucleus of the nearby galaxy NGC 628 (M74). Its progenitor has been identified by Van Dyk et al. (2003) and Smartt et al. (2004) as an $8_{-2}^{+4}M_{\odot}$ red supergiant. Its photometric and spectral evolution are very similar to the type II-plateau (II-P) SN 1999em (Hendry et al. 2005, hereafter H05), from which Van Dyk et al. (2003) identify SN 2003gd as a type II-P, while H05 have estimated the reddening as $E(B-V) = 0.14 \pm 0.06$ (of which 0.07 mags are Galactic, Schlegel, Finkbeiner & David 1998), and the distance to M74 as 9.3 ± 1.8 Mpc. Both groups conclude the SN was discovered roughly 87 days after explosion, which therefore occurred around 2004 Mar 17.

Since the SN exploded near a spiral arm in M74, it is expected to illuminate surrounding material in the form of scattered-light echoes. Light echoes offer one of the most effective means to probe circumstellar and interstellar structure. As an example, echoes from SN 1987A have been used to map the surrounding circumstellar (Sugerman et al. 2005b) and interstellar (Xu, Crotts & Kunkel 1995) media, thereby probing the progenitor's mass-loss history, its location within its galaxy, and the structure and history of the associated stars and gas. For recent reviews on light echoes, see Sugerman (2003) and Patat (2005).

To date, resolved echoes have been reported around only four supernovae: SN 1987A (Crotts 1988), SN 1991T (Schmidt et al. 1994; Sparks et al. 1999), SN 1993J (Sugerman & Crotts 2002; Liu et al. 2003), and SN 1998bu (Cappellaro et al. 2001). This *Letter* presents the discovery and preliminary geometric and compositional analyses of a new light echo around SN 2003gd.

2. OBSERVATIONS AND REDUCTIONS

Three epochs of publically-available data were accessed in the *Hubble Space Telescope* (*HST*) archive. The progenitor of SN 2003gd was serendipitously observed on the Wide Field 2 chip of the Wide Field and Planetary Camera 2 (WFPC2) in the F606W filter on 2002 Aug 25 and 28, with total exposure

time of 3100 sec. The SN was observed with the Advanced Camera for Surveys (ACS) High Resolution Camera (HRC) on 2003 Aug 1 (day 137 after outburst), and again on 2004 Dec 8 (day 632). The SN is too bright in the former epoch to be reliably PSF subtracted, thus these earlier data were of limited use. In 2004, the SN was imaged in the F435W and F625W filters, with total integration times of 840 and 350 sec, respectively.

Pipeline-calibrated data were first filtered to mask warm pixels by rejecting single pixels that deviated by more than 3σ from the variance of the other 8 pixels in a 9-pixel moving box. Individual exposures were combined using the `multidrizzle` task within `stsdas` to reject cosmic rays and perform geometric-distortion corrections. The WFPC2 data were drizzled with a final pixel scale of $0.''065$ pix $^{-1}$, to increase the resolution of the PSF.

To intercompare images, HRC data were geometrically-registered to a common orientation using a shift, rotation, and scaling. The F625W HRC image from 2004 was drizzled to $0.''065$ pix $^{-1}$ and registered to the WFPC2 field using a second-order polynomial. All registrations had residuals < 0.1 pixel rms. HRC data, and the WFPC2 F606W and HRC F625W images, were PSF-matched, photometrically scaled, and subtracted using the `difimphot` image-subtraction techniques of Tomaney & Crotts (1996), as described in Sugerman et al. (2005a), using Tiny Tim model PSFs that underwent identical geometric transformations.

Photometric calibrations were adopted from the image headers, and unless otherwise noted, magnitudes are expressed in STMAGS. Conversion to Johnson/Cousins magnitudes was accomplished as specified in Sirianni et al. (2005). For example, PSF-fitted photometry of the SN in 2004 yields $m_{F435W} = 23.39 \pm 0.13$ and $m_{F625W} = 23.67 \pm 0.12$, which translate into $B = 23.98 \pm 0.15$ and $R = 23.13 \pm 0.16$. Note that the transformations, while color dependent, are determined from stellar sources, and since they do not account for the strong emission lines present in a SN spectrum, the uncertainties are likely to be larger than the formal errors quoted.

3. ECHO IDENTIFICATION AND GEOMETRY

Figure 1a shows the ACS/HRC F435W image from 2004. An arc of flux is present between $0.''23$ and $0.''38$ from the SN, between PA 260° – 340° , as well as a few isolated, point-

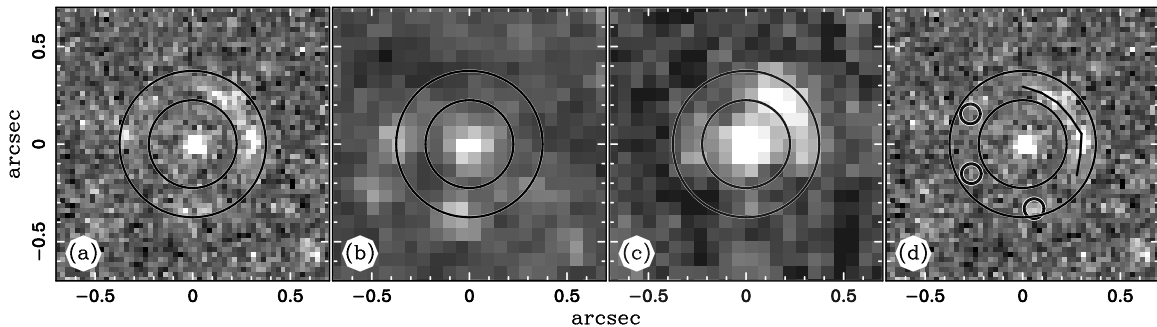


FIG. 1.— *HST* images of a $1''.4$ field surrounding SN 2003gd. North is up and east is left. The SN (or progenitor) is at the center of each frame. Circles of radii $0''.225$ and $0''.375$ roughly delimit the radial extent of the echoes. (a) ACS/HRC F435W image from 2004. (b) WFPC2 F606W image of the progenitor, drizzled to $0''.065 \text{ pix}^{-1}$. (c) PSF-matched difference image between the ACS/HRC F625W data from 2004 drizzled to $0''.065 \text{ pix}^{-1}$, and the data in panel b. (d) Panel a with the neighboring stars removed. The bright echo loci are marked with a black line, while fainter echo positions are denoted with small black circles.

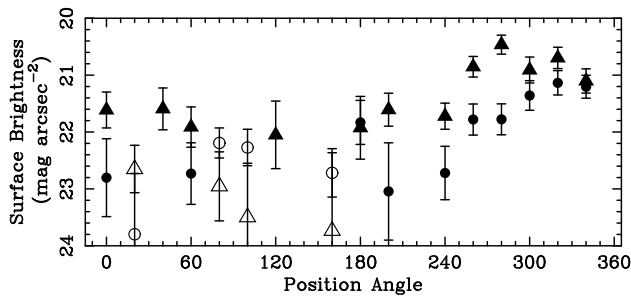


FIG. 2.— Surface brightness measured in 20° wedges in PA from $\rho = 0''.23$ to $0''.38$ in F435W (triangles) and F625W (circles). Filled symbols denote position angles at which echoes were identified.

source like features at other position angles. A comparison with the WFPC2 F606W image from 2002 (panel b) shows that two of these sources are nearby stars, yet there is no observable arc of flux northwest of the SN.

The exposure time of the F625W HRC image from 2004 is short compared to the F606W WFPC2 integration, making the HRC image very noisy at its native resolution. However, once resampled to the WFPC2 resolution, this image was successfully PSF-matched to and differenced from the WFPC2 data, as shown in panel (c). The nearby stars have cleanly subtracted away, revealing the bright arc to the northwest, and potential sources at PAs 60° , 100° , and 190° . The bright arc is consistent with a scattered-light echo, while the nature of these isolated sources (i.e., echoes from more localized density enhancements versus detector artifacts) is unclear.

The positions of the three companion stars were measured on the WFPC2 frame and transformed to the ACS coordinate system, then subtracted away from the 2004 data using Tiny Tim model PSFs and the *daophot* package. The result in F435W is shown in panel (d). To measure the positions of the echoes, and to search for faint flux not readily apparent to the eye, radial profiles of angular width 20° were inspected, and peaks were fit with moffat profiles to find the center and width of any extended features (Sugerman et al. 2005a). All identified echo sources have been marked in panel (d). The bright arc extends from $0''.28$ to $0''.32$, with coherent signal detected from PA 250° – 360° . Adopting a distance of 9.3 Mpc , these correspond to separations on the sky of $\rho = 41$ – 47 lt-yr^1 .

¹ With units of years and light-years, the echo equations simplify considerably since $c = 1$, hence the somewhat unorthodox use of distances in lt-yr

The surface brightnesses of the echoes as measured in annuli with 20° arclength are plotted in Fig. 2. For echoes already identified above, the moffat-profile width was used as the annular width, while at all other PAs the annuli were at $0''.28$ and $0''.32$. In general, the fluxes of identified echoes track each other across PA, however there is considerable scatter due to the low signal-to-noise of these short observations. Echoes between PA 0° – 240° are considered candidates at this time since their detections are only marginal; in some cases the echo was not even detected in F625W.

As noted in §1, SN 2003gd was discovered ~ 87 days after explosion. However, H05 have argued it is sufficiently similar to SN 1999em to warrant using the latter’s photometry and spectra as surrogates at earlier times. Filling in the first ~ 80 days of photometry with that of SN 1999em (H05 and references therein), the SN 2003gd light curves have roughly 120 day plateaus, peaking very early in blue and around 60 days in the red. Unfortunately, ACS spatial resolution cannot differentiate the temporal color peaks in these echoes, as seen in echoes around N V838 Mon (Bond et al. 2003).

If we assume maximum light occurred around 60 days, the line-of-sight distance of each echo is computed as $z = \rho^2 / (2ct) - ct/2$, where t is the time since maximum light. The center of the bright arc therefore lies between 530 and 650 lt-yr in front of the SN, while the other possible echoes extend up to $z = 780 \text{ lt-yr}$. Using the naming scheme of Xu et al. (1995), we label the bright arc NW600.

The three-dimensional positions of the echoes have been rendered in Figure 3 using the techniques described in Sugerman et al. (2005a) and briefly annotated in the figure caption. Panel (a) shows the positions from Fig. 1d as viewed on the plane of the sky. From the side (panel b), the echo points appear to lie along a steeply-inclined plane, with its normal inclined roughly 60° to the line of sight at PA 340° . This is shown in the oblique view of panel (e).

As shown in Fig. 2 of Sugerman (2003), an echo has a width $\Delta\rho$ resulting from a convolution of the depth of the material Δz and the finite duration of the light pulse Δt . Using the widths measured during radial-profile fitting, and Eq. (11) of Sugerman (2003), the depths of the echoes are 110–160 lt-yr. The spatial extent of each echo measurement has been shown in Fig. 3c, where each point in the panel (b) is replicated through its range of Δz and position angle.

While panel (c) is still suggestive of a highly-inclined plane, the case for this structure becomes less compelling when the

throughout this paper.

TABLE 1
DUST MODELING RESULTS

Model	a_{max} μm	n_H (cm^{-3})			$A_V/\Delta z_{100}^a$		
		C	Si	C+Si	C	Si	C+Si
WD01 ^a	0.25	...	1.3	1.1	...	0.033	0.050
	0.13	30.	0.38
MRN ^b	0.25	...	2.3	1.5	...	0.037	0.083
	0.13	15.	0.40

^amags per 100 lt-yr of material in z .

^bWeingartner & Draine (2001) Galactic dust with $R_V = 3.1$ and $b_C = 6 \times 10^{-5}$.

^cMathis, Rumpel, & Nordsieck (1977) dust with $n(a) \propto a^{-3.5}$

light grey points (echo candidates) are ignored. Consider also Fig. 3d and f, which show the three-dimensional positions of all image pixels that are part of the northwestern arc. From the side, this locus appears consistent with a thick ($\Delta z = 300\text{--}400$ lt-yr) sheet of material that is roughly perpendicular to the line of sight. This underscores the fundamental problem that it is very difficult to identify the geometry of an echoing structure with a single epoch of observation.

4. DUST ANALYSIS

When echoes are observed in multiple wavebands, characteristics of the scattering dust (i.e. dust composition, grain size, and density) can be constrained by comparing the SN and echo photometry, using e.g. the formalisms presented in Sugerman (2003). Since the SN 2003gd echoes were observed in only two filters, and since the signal-to-noise of the observations is low, such analyses have limited accuracy. In particular, with only two wavebands, a variety of dust mixtures may fit the data equally well (see Patat 2005). As such, only the total surface brightnesses of the NW600 echo are considered, which are $\mu_{F435W} = 20.8 \pm 0.2$ and $\mu_{F625W} = 21.4 \pm 0.3$ mags arcsec⁻¹.

The light curves of SN 1999em and 2003gd (H05 and references therein) integrated over the first 140 days yield B , V , and R fluences of $(7.0, 8.0, 7.0) \times 10^{-8}$ ergs cm⁻² Å⁻¹, respectively. When integrated over the first 140 days, the spectra of SN 1999em² corrected for extinction toward SN 2003gd match these to better than 1%, yielding fluences of 6.5×10^{-8} and 7.5×10^{-8} ergs cm⁻² Å⁻¹ in F435W and F625W.

Comparison of the echo surface brightness to the SN fluence yields a color shift of $\Delta(m_{F435W} - m_{F625W}) = -0.8 \pm 0.4$. Two extremal color shifts are for Galactic (Weingartner & Draine 2001) and Rayleighian³ dust, which using the scattering function $S(\lambda, \mu)$ of Sugerman (2003) yields $\Delta(m_{F435W} - m_{F625W}) = -0.3$ and -1.2 , respectively. This rules out purely Rayleighian particles, suggesting instead that the dust is similar to Galactic dust, but with smaller maximum grain sizes.

A more detailed comparison of the echo surface brightness to a range of dust models (Sugerman 2003) yields the results summarized in Table 1. Each model used the dust properties in the first column, with minimum grain size $a_{min} = 5 \times 10^{-4} \mu\text{m}$, and maximum grain size given in column 2. The associated gas density n_H and resulting extinction are given

² Acquired from the SUSPECT supernova spectrum archive, <http://suspect.nhn.ou.edu>.

³ Only small-particles, hence scattering efficiency $\propto \lambda^{-4}$

for purely carbonaceous (C), purely silicate (Si), and a Galactic mixture (C+Si) of dust. A Galactic dust composition with $a_{max} \sim 0.25 \mu\text{m}$ and $n_H \sim 1\text{--}2 \text{ cm}^{-3}$ is a good fit to the echoes, while slightly-higher densities are required for Si dust. By contrast, C dust requires smaller grains and at least an order of magnitude more dust.

An additional constraint is provided by the reddening H05 measure to the SN (§1), which for $R_V = 3.1$ and with 0.07 mag of Galactic extinction removed, yields $A_V = 0.36$. C dust is only realistic if the echoes occur in a thin sheet of material. Similarly, Si dust requires a sheet at least twice as thick as actually observed. Assuming the scattering occurs in a sheet roughly 300–400 lt-yr thick, the echoes are reasonably-well fit by the Galactic composition. However, a better fit may require a higher proportion of small carbon grains than are found in Galactic dust. For example, 75% carbon grains with $a_{max} = 0.15 \mu\text{m}$ and 25% silicate grains with $a_{max} = 0.25 \mu\text{m}$ yield a gas density of 2.2 cm^{-3} and $A_V/\Delta z_{100} = 0.078$, which satisfies the observed extinction for a slab of dust 400 lt-yr thick. Again, since the echoes have only been measured at two wavebands, these specific results are far from conclusive.

5. DISCUSSION

The disk of M74 is inclined $8^\circ \pm 5^\circ$ at PA $23^\circ \pm 6^\circ$ (Garcia-Gomez & Athanassoula 1991) with a scale height of 730 ± 200 lt-yr (Peng 1988). As discussed in §3, there are two hypotheses for the geometry of the echoing dust. The thick slab with shallow inclination is consistent with the geometry of the disk, and a density of $1\text{--}2 \text{ cm}^{-3}$ is consistent with ambient density of the Galactic interstellar medium. In this case, the SN has illuminated the disk of M74, and is itself located behind the disk. On the other hand, a thinner, highly-inclined plane of dust might delineate the shell of a (remnant) superbubble blown from a nearby OB association of stars (See for example Xu et al. 1995). A blue cluster of stars with integrated color of $B - V = -0.25$ is located about $3''$ from the SN at PA 65° . Alternatively, there are at least two additional blue clusters of stars within $12''$ of the SN, all of which may have formed a complex network of bubbles in front of (or around) SN 2003gd. Obviously, additional observations are required to properly understand the geometry of this material.

Adopting the thick-sheet model, this echo will expand at $d\rho/dt = c(z+ct)/\rho = 0.1 \text{ yr}^{-1}$. Thus, observations should continue at yearly intervals. The observed echo is only a $\sim 90^\circ$ arc, with scattered hints of echoes that form a more complete loop around the SN. Since the exposure times of the 2004 ACS data were short, it is unclear whether fainter echo flux is present at all position angles. Future integrations should probe at least one magnitude deeper, and should include the complete $U - I$ range to properly study the dust characteristics.

The total echo fluxes are 4.0×10^{-16} and 2.6×10^{-16} ergs cm⁻² s⁻¹ in the F435W and F625W filters, respectively, corresponding to $B = 24.2 \pm 0.1$ and $R = 23.9 \pm 0.1$ mag. Using the same scattering codes as above, these yield a V -band magnitude of 24.2 ± 0.2 . Around day 137 (the 2003 August ACS observations), the echo was at $\rho = 0.1$ but only 2% brighter. Compared to the SN fluxes of 19.1, 17.4, and 16.3 in B , V , and R respectively (H05), the echo was at least 5 mag fainter and therefore lost within the wings of the possibly-saturated PSF. However, a small correction must be made to earlier photometry to remove any echo contributions.

As a final note, H05 report photometry of the SN from day 493 as $B = 21.76 \pm 0.06$ and $R = 20.59 \pm 0.09$ mags. They further speculate that dust may be forming in the ejecta of the

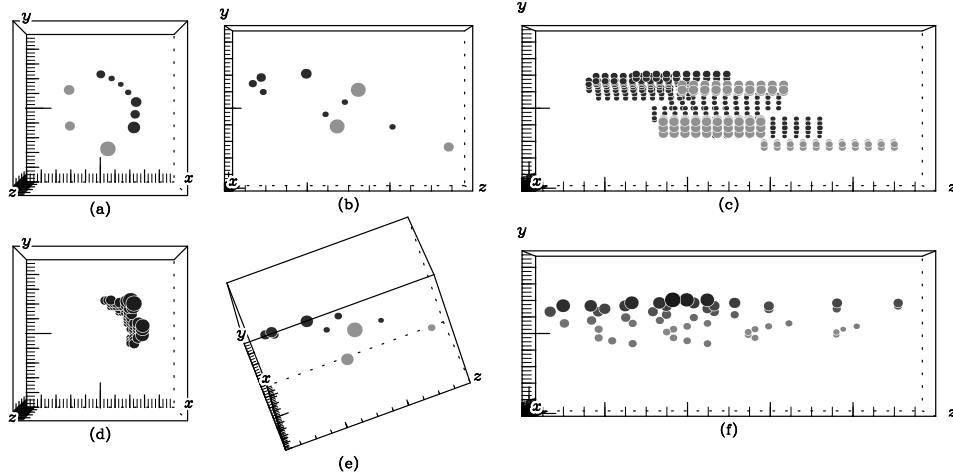


FIG. 3.— Three-dimensional renderings of the observed echo locations. Axes are defined with x increasing west, y increasing north, and z increasing toward the observer. Axis labels denote the direction of increasing value. Along the x and y axes, major ticks mark 20 lt-yr, while in z major ticks mark 100 lt-yr; the longest ticks mark the origin. The coordinates and axes have been given a slight perspective transformation, and larger point size indicates closer position to the view. Dark points denote the bright echo arc (NW600) from PA 250° – 360° , with the other echoes marked in light grey. The z axes run from 500 to 800 lt-yr in panels (b)–(c), and from 400–900 lt-yr in panels (d)–(e). (a) Face-on view as observed on the sky. These data are also shown (b) from the side (rotated 90°) with the observer to the right, and (d) from an oblique view, in which echoes appear to lie roughly along a plane. (c) As panel b, but showing the spatial extent of dust along the line of sight (z) and in position angle that comprises each individual echo position. All pixels from the 2004 ACS data belonging to NW600 are rendered (d) face on, and (f) from the side. In panel (f), points are shaded using simple ray tracing assuming a single light source behind the reader.

SN, resulting from a small blueshift in $H\alpha$ emission, and a marginally-significant drop in this late-time photometry. Following Turatto et al. (1990), the average Type IIP decay rates for these filters are roughly 0.7 and 1.0 mags per 100 days, yielding expected B and R values of 22.7 and 22.0. Compared to those measured on day 632, the photometry has decreased about 1.3 and 0.9 mags in B and R , consistent with an increase in the extinction toward the SN of $\Delta A_V = 1$ mag, and further consistent with dust formation at these late times (see also Wooden et al. 1993).

Sincere thanks to Steve Lawrence and the referee, Fernando Patat, for their careful reading of this manuscript. This work was based on observations made with the NASA/ESA Hubble Space Telescope, obtained from the Data Archive at the Space Telescope Science Institute, which is operated by the Association of Universities for Research in Astronomy, Inc., under NASA contract NAS 5-26555. This research was supported by STScI grants 10204 and 82301.

REFERENCES

- Bond, H. E., et al. 2003, *Nature*, 422, 405
 Cappellaro, E. et al. 2001, *ApJ*, 549, L215
 Crotts, A. 1988, *IAUC*, 4561
 Elmhamdi, A., et al. 2003, *MNRAS*, 338, 939
 Evans, R., & McNaught, R. H. 2003, *IAU Circ.*, 8150, 2
 Garcia-Gomez, C., & Athanassoula, E. 1991, *A&AS*, 89, 159
 Hamuy, M., et al. 2001, *ApJ*, 558, 615
 Hendry, M. A., et al. 2005, *MNRAS*, 359, 906 (H05)
 Liu, J.-F., Bregman, J. N., & Seitzer, P. 2003, *ApJ*, 582, 919
 Mathis, J. S., Ruml, W., & Nordsieck, K. H. 1977, *ApJ*, 217, 425
 Patat, F. 2005, *MNRAS*, 357, 1161
 Peng, Q.-H. 1988, *A&A*, 206, 18
 Smartt, S. J., Maund, J. R., Hendry, M. A., Tout, C. A., Gilmore, G. F., Mattila, S., & Benn, C. R. 2004, *Science*, 303, 499
 Sirianni, M., et al. 1005, *PASP*, accepted (astro-ph/0507614)
 Schlegel, D. J., Finkbeiner, D. P., & Davis, M. 1998, *ApJ*, 500, 525
 Schmidt, B.P. et al. 1994, *ApJ*, 424, L19
 Shostak, G. S., & van der Kruit, P. C. 1984, *A&A*, 132, 20
 Sparks, W.B. et al. 1999, *ApJ*, 523, 585
 Sugerman, B.E.K. 2003, *AJ*, 126, 1939
 Sugerman, B. E. K., & Crotts, A. P. S. 2002, *ApJ*, 581, L97
 Sugerman, B. E. K., Crotts, A. P. S., Kunkel, W. E., Heathcote, S. R., & Lawrence, S. S. 2005a, *ApJS*, 159, 60
 Sugerman, B. E. K., Crotts, A. P. S., Kunkel, W. E., Heathcote, S. R., & Lawrence, S. S. 2005b, *ApJ*, 627, 888
 Tomaney, A., & Crotts, A. P. S. 1996, *AJ*, 112, 2872
 Turatto, M., Cappellaro, E., Barbon, R., della Valle, M., Ortolani, S., & Rosino, L. 1990, *AJ*, 100, 771
 Van Dyk, S. D., Li, W., & Filippenko, A. V. 2003, *PASP*, 115, 1289
 Weingartner, J. C. & Draine, B. T. 2001, *ApJ*, 548, 296
 Wooden, D. H. et al. 1993, *ApJS*, 88, 477
 Xu, J., Crotts, A.P.S. & Kunkel, W.E. 1995, *ApJ*, 451, 806 (Erratum: 463, 391)